

Short range order in a steady state of irradiated Cu-Pd alloys: Comparison with fluctuations at thermal equilibrium

I. Tsatskis[†] and E. K. H. Salje

Department of Earth Sciences, University of Cambridge, Downing Street, Cambridge CB2 3EQ, United Kingdom

The equilibrium short-range order (SRO) in Cu-Pd alloys is studied theoretically. The evolution of the Fermi surface-related splitting of the (110) diffuse intensity peak with changing temperature is examined. The results are compared with experimental observations for electron-irradiated samples in a steady state, for which the temperature dependence of the splitting was previously found in the composition range from 20 to 28 at.% Pd. The equilibrium state is studied by analysing available experimental and theoretical results and using a recently proposed alpha-expansion theory of SRO which is able to describe the temperature-dependent splitting. It is found that the electronic-structure calculations in the framework of the Korringa-Kohn-Rostoker coherent potential approximation overestimate the experimental peak splitting. This discrepancy is attributed to the shift of the intensity peaks with respect to the positions of the corresponding reciprocal-space minima of the effective interatomic interaction towards the (110) and equivalent positions. Combined with an assumption about monotonicity of the temperature behaviour of the splitting, such shift implies an increase of the splitting with increasing temperature for all compositions considered in this study. The alpha-expansion calculations seem to confirm this conclusion.

05.50+q, 64.60.Cn, 61.66.Dk, 71.18+y

I. INTRODUCTION

Almost a decade ago, Kulik *et al.*¹ published their experimental results on electron diffraction from irradiated Cu-Pd alloys. In that study samples with 20, 22, 24 and 28 at.% Pd were maintained by high-energy electron irradiation in a steady disordered state away from their thermal equilibrium state at temperatures between 200 and 400 K. At these temperatures and compositions equilibrium Cu-Pd alloys exhibit long-range order; the disordered state occurs only at much higher temperatures. In the equilibrium disordered state the intensity of diffuse scattering from Cu-Pd alloys with more than about 15 at.% Pd is characterised by the fourfold splitting of intensity peaks located at the (100), (110) and equivalent positions in the reciprocal space.^{1–7} The resulting diffuse intensity distribution has maxima at the (1q0) and equivalent positions (Fig. 1); the value of q increases with increasing Pd concentration. This fine structure of diffuse scattering is caused by the atomic short-range order (SRO) and is a result of the indirect interaction of alloy atoms through conduction electrons in a situation when an alloy has reasonably well-defined Fermi surface with relatively flat areas.^{8,9} In this case the corresponding minima of the effective pair interatomic interaction in the reciprocal space are also split, and their separation is related to the wavevector $2\mathbf{k}_F$ which spans these flat areas of the Fermi surface.

Similar splitting of the diffuse intensity peaks was observed in the nonequilibrium steady disordered state under irradiation.¹ In addition to the expected concentration dependence of q , its variation with irradiation temperature was found. Even more curious was the qualitative change of the temperature dependence of the splitting with concentration: q decreased with increasing temperature in the case of 20, 22 and 24 at.% Pd, but this

trend was reversed for the alloy with 28 at.% Pd for which an increase of the peak separation with temperature was found. At the same time, there was an increase of the scattering intensity with increasing temperature for all four compositions, contrary to the case of alloys at equilibrium where the intensity decreases with increasing temperature. A qualitative explanation of the temperature dependence of the splitting was proposed as follows. Firstly, the behaviour of the equilibrium SRO diffuse intensity in the case of the exactly solvable one-dimensional Ising model with competing antiferromagnetic nearest- and next-nearest-neighbour interactions was studied. It turned out that the peak positions varied with temperature. This result is in contrast with the mean-field-related Krivoglaz-Clapp-Moss (KCM) treatment^{8,10} which predicts temperature-independent peak positions at the minima of the interaction. As the intensity increased with decreasing temperature, the peak positions shifted towards the wavevector of the corresponding ground state. A similar result was obtained earlier for the two-dimensional ANNNI model using the cluster variation method.¹¹ It was concluded that the temperature dependence of the peak positions is a phenomenon which cannot be understood in the framework of mean-field theory. Secondly, the assumption was made that the behaviour of the diffuse intensity in irradiated Cu-Pd alloys was analogous to that of the equilibrium one-dimensional model. The only qualitative difference between the two cases was the opposite roles played by temperature. Based on this “inverse temperature hypothesis”, the conclusion was drawn that one might expect to find the increase in q with temperature for the Cu-Pd alloy system at equilibrium. Here it may be added that the reversal of the temperature behaviour of the peak splitting could be expected according to this hypothesis as concentration increases, from the increase with tem-

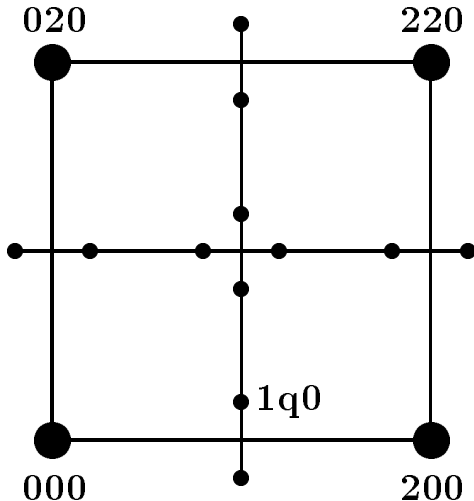


FIG. 1. Schematic reciprocal-space picture of scattering from disordered Cu-Pd alloys. Large dots represent the Bragg reflections. Small dots correspond to the split diffuse intensity peaks.

perature for 20, 22 and 24 at.% Pd to the decrease for 28 at.% Pd.

Last year, such an increase of the peak separation with temperature was observed at equilibrium by Reichert *et al.*¹² for the disordered Cu₃Au alloy. Moss and Reichert^{13,14} found the same behaviour by analysing the Monte Carlo simulation results of Roelofs *et al.*¹⁵ for the Cu-14.4 at.% Al alloy. In the latter work the inverse Monte Carlo pair interactions were determined from the experimental diffuse intensity at a single temperature and subsequently used to generate the Monte Carlo intensities at other temperatures. The theory of the temperature dependence of the splitting was proposed by Tsatskis;^{14,16} it identifies the wavevector dependence of the self-energy of the pair correlation function (PCF) as the origin of this effect. The self-energy $\Sigma(\mathbf{k})$ and the interaction term $2\beta V(\mathbf{k})$ enter the expression for the SRO diffuse intensity on an equal footing (Eq. (2.1a) below). In the KCM approximation the fact that the self-energy is a function of \mathbf{k} is ignored. Apart from the observed increase in q with temperature, the possibility of the opposite behaviour, i.e., the decrease of the peak separation as temperature increases, was predicted. This is exactly what should be expected under equilibrium conditions for the Cu-28 at.% Pd alloy, if the inverse temperature hypothesis is valid, although such temperature dependence was never seen experimentally. The possibility of the reversal of the temperature dependence of the peak splitting with increasing concentration seems to be indicated also by the results of the Monte Carlo simulations of Ozolinš *et al.*¹⁷ for the first-principles alloy Hamiltonian with pair and multiatom interactions (25 at.% Pd) and the X-ray scattering measurements of Reichert *et al.*⁷ (29.8 at.% Pd). In both cases no (or a very small) change of the

splitting with changing temperature was found.

The idea of the present study is to gain further insight into the behaviour of Cu-Pd alloys under irradiation by studying theoretically the evolution of the diffuse peak splitting with changing temperature in these alloys at equilibrium. More exactly, the aim is to find out whether the splitting increases with temperature in the range from 20 to 24 at.% Pd as the inverse temperature hypothesis implies and whether this behaviour is reversed as concentration increases to 28 at.% Pd. Starting from the experimental SRO diffuse intensity measured at a particular temperature, we first solve the inverse scattering problem and calculate the effective interaction which is assumed to be pairwise and temperature-independent. Then the direct problem is solved and the self-energy and diffuse intensity at different temperatures are calculated. The underlying theory of SRO is described in Sec. II. Sec. III considers data for Cu-Pd alloys existing in the literature. Finally, the results are discussed in Sec. IV.

II. ALPHA-EXPANSION THEORY OF SRO

We start by describing the theory of SRO which leads to the temperature-dependent peak splitting and is used in Sec. IV to relate the SRO diffuse intensities at different temperatures. This theory is based on the alpha-expansion (AE) for the self-energy;¹⁶ the self-energy is the only unknown quantity in the otherwise formally exact expression for the SRO intensity. The AE is the expansion in powers of SRO parameters α_{lmn} , hence the name. It was proposed as a generalisation of another approach to the calculation of the self-energy, the gamma-expansion method (GEM),^{18–20} to deal with distant interactions which are essential in the case of the Fermi surface-related splitting. The complete set of the AE equations has the form

$$I_{SRO}(\mathbf{k}) = \frac{1}{c(1-c) [-\Sigma(\mathbf{k}) + 2\beta V(\mathbf{k})]} , \quad (2.1a)$$

$$\Sigma(\mathbf{k}) = \Sigma_{000} + \sum_{lmn \neq 000} Z_{lmn} \Sigma_{lmn} \lambda_{lmn}(\mathbf{k}) , \quad (2.1b)$$

$$\Sigma_{lmn} = a\alpha_{lmn}^2 + b\alpha_{lmn}^3 , \quad lmn \neq 000 , \quad (2.1c)$$

$$\alpha_{000} = \frac{1}{\Omega} \int d\mathbf{k} I_{SRO}(\mathbf{k}) = 1 , \quad (2.1d)$$

$$\alpha_{lmn} = \frac{1}{\Omega} \int d\mathbf{k} I_{SRO}(\mathbf{k}) \lambda_{lmn}(\mathbf{k}) . \quad (2.1e)$$

In Eqs. (2.1) \mathbf{k} is the wavevector, $I_{SRO}(\mathbf{k})$ is the SRO diffuse intensity in Laue units, c is the concentration, $\Sigma(\mathbf{k})$ is the self-energy of the PCF G (the latter is defined by Eq. (2.6) below), $\beta = 1/T$, T is the temperature in energy units, and $V(\mathbf{k})$ is the Fourier transform of the pair ordering potential

$$V_{ij} = \frac{1}{2} (V_{ij}^{AA} + V_{ij}^{BB}) - V_{ij}^{AB} . \quad (2.2)$$

The potential $V_{ij}^{\alpha\beta}$ corresponds to the interaction between an atom of type α at site i and an atom of type β at site j . Further, α_{lmn} , Σ_{lmn} , Z_{lmn} and

$$\lambda_{lmn}(\mathbf{k}) = Z_{lmn}^{-1} \sum_{\mathbf{r} \in lmn} \exp(i\mathbf{kr}) \quad (2.3)$$

are the SRO parameter, matrix element of the self-energy, coordination number and shell function for the coordination shell lmn , respectively, while α_{000} and Σ_{000} are the corresponding diagonal matrix elements. The summation in Eq. (2.1b) is performed over all coordination shells, whereas that in Eq. (2.3) is over the lattice vectors \mathbf{r} belonging to the coordination shell lmn . The integration in Eqs. (2.1d) and (2.1e) is carried out over the Brillouin zone of volume Ω . Coefficients a and b in Eq. (2.1c) are functions of concentration,

$$a = \frac{(1-2c)^2}{2[c(1-c)]^2}, \quad (2.4a)$$

$$b = \frac{[1-6c(1-c)]^2 - 3(1-2c)^4}{6[c(1-c)]^3}. \quad (2.4b)$$

The SRO parameters α are proportional to the corresponding matrix elements of the PCF G ,

$$G_{ij}^{AA} = G_{ij}^{BB} = -G_{ij}^{AB} = c(1-c)\alpha_{ij}, \quad (2.5)$$

the definition of the PCF being

$$G_{ij}^{\alpha\beta} = \langle p_i^\alpha p_j^\beta \rangle - \langle p_i^\alpha \rangle \langle p_j^\beta \rangle, \quad (2.6)$$

where p_i^α is the occupation number,

$$p_i^\alpha = \begin{cases} 1, & \text{atom of type } \alpha \text{ at lattice site } i, \\ 0, & \text{otherwise,} \end{cases} \quad (2.7)$$

and angular brackets denote statistical averaging.

The meaning of Eqs. (2.1) is as follows. The first of Eqs. (2.1d) and Eq. (2.1e) are the consequences of the fact that α_{ij} is the back Fourier transform of the intensity $I_{SRO}(\mathbf{k})$. Eq. (2.1b) is the relation between the direct- and reciprocal-space representations of the self-energy. Eqs. (2.1b) and (2.1e) are written in coordination shell notations. The second of Eqs. (2.1d) is the well-known sum rule²¹ which reflects the property

$$p_i^\alpha p_i^\beta = p_i^\alpha \delta^{\alpha\beta} \quad (2.8)$$

of the occupation numbers following from their definition (2.7). The less obvious Eq. (2.1a) is one of the possible forms of the Dyson equation²² which is satisfied by the PCF (2.6); this issue is discussed in considerable detail elsewhere.²³ The key equation is Eq. (2.1c) which closes the set of Eqs. (2.1) by expressing the off-diagonal part of the self-energy in terms of the SRO parameters. Its right-hand side is, in fact, two first non-zero terms of a series expansion of Σ_{lmn} in powers of the SRO parameters. The latter are almost always sufficiently small,

which justifies the expansion. These two terms were previously calculated^{19,20} in the framework of the GEM using self-consistent renormalization of the bare propagator $(\beta V)^{-1}$ in the generating functional for correlation functions.¹⁸ The resulting expansion for the matrix elements of the self-energy was in powers of the matrix elements of the fully dressed propagator. This propagator is the PCF (2.6), and its matrix elements are therefore proportional to the corresponding SRO parameters. Thus, Eqs. (2.1) form the set of self-consistent equations for the matrix elements of the self-energy (alternatively, Σ_{000} and α_{lmn} , $lmn \neq 000$, can be used as independent variables) and constitute the closed-form approximation for SRO. A particular AE approximation is defined by using Eq. (2.1c) for only a finite number of coordination shells and neglecting all other matrix elements of the self-energy. Another sequence of the AE approximations can be generated in the same way by taking into account only the lowest-order (quadratic) term in the AE expansion for Σ_{lmn} and ignoring the third-order contribution. For the rest of the paper both terms (as in Eq. (2.1c)) will be used. The AE is expected to be at least as accurate as the GEM, and the latter was used successfully in dealing with both direct and inverse diffuse scattering problems,^{19,20,24} providing reliable results at almost all temperatures. The zero-order approximation of the AE is the well-known spherical model (SM) for correlations,²⁵ also known under the name of the Onsager cavity field theory.²⁶ In the SM the self-energy is diagonal, i.e., wavevector-independent; the single non-zero matrix element Σ_{000} is a function of temperature and concentration and is determined from the sum rule (2.1d).

In order to use Eqs. (2.1) for calculating the evolution of the diffuse intensity with temperature and, in particular, the temperature dependence of the peak splitting, it is necessary to have information about the interaction V . It is assumed here that the interaction does not depend on temperature in the relevant temperature intervals; on the other hand, it is clearly concentration-dependent, so that a separate interaction set is needed for each alloy composition. We start from the set of the experimental SRO parameters and calculate the AE interaction in the reciprocal space by solving the inverse diffuse-scattering problem.^{19,20} This interaction can then be used for calculation of diffuse intensities at different temperatures and possibly, with much less confidence, at slightly different concentrations.

To solve the inverse problem, we rewrite Eq. (2.1a) as an expression for the interaction:

$$V_{AE}(\mathbf{k}) = \frac{T}{2} \left[\frac{I_{SRO}^{-1}(\mathbf{k})}{c(1-c)} + \Sigma(\mathbf{k}) \right]. \quad (2.9)$$

The SRO diffuse intensity here is recalculated from the set of the experimental SRO parameters:

$$I_{SRO}(\mathbf{k}) = 1 + \sum_{lmn \neq 000} Z_{lmn} \alpha_{lmn} \lambda_{lmn}(\mathbf{k}). \quad (2.10)$$

In Eq. (2.10) the sum rule (2.1d) was used; otherwise, it is just the Fourier transformation written in coordination shell notations, similar to Eq. (2.1b). Substitution of Eqs. (2.1b) and (2.1c) into Eq. (2.9) shows that the only quantity in the resulting expression for $V_{AE}(\mathbf{k})$ which is needed to be expressed in terms of the SRO parameters (or, equivalently, the SRO intensity) is the diagonal part Σ_{000} of the self-energy. The off-diagonal part of Σ is already an explicit function of the SRO parameters (Eq. (2.1c)). To find Σ_{000} , we integrate Eq. (2.9) over the Brillouin zone; this integration gives the diagonal direct-space matrix element of the integrand, as in Eq. (2.1d). The interaction V is an off-diagonal matrix in the direct space because of the absence of the self-interaction. Therefore, after the integration the left-hand side of Eq. (2.9) is zero and, as a result,

$$\Sigma_{000} = -\frac{\langle I_{SRO}^{-1} \rangle}{c(1-c)}, \quad (2.11a)$$

$$\langle I_{SRO}^{-1} \rangle = \frac{1}{\Omega} \int d\mathbf{k} I_{SRO}^{-1}(\mathbf{k}). \quad (2.11b)$$

Thus, Eq. (2.9) for the AE interaction can be written as

$$V_{AE}(\mathbf{k}) = V_{SM}(\mathbf{k}) + \frac{T}{2} \Sigma_{od}(\mathbf{k}), \quad (2.12)$$

where $\Sigma_{od}(\mathbf{k})$ is the Fourier transform of the off-diagonal part of the self-energy defined by Eq. (2.1c), and

$$V_{SM}(\mathbf{k}) = \frac{T}{2c(1-c)} [I_{SRO}^{-1}(\mathbf{k}) - \langle I_{SRO}^{-1} \rangle] \quad (2.13)$$

is the interaction obtained in the framework of the SM, i.e., in the zero-order AE approximation in which the off-diagonal part of the self-energy is zero. Note that, when compared with the interaction resulting from the KCM expression for $I_{SRO}(\mathbf{k})$,^{8,10}

$$V_{KCM}(\mathbf{k}) = \frac{T}{2c(1-c)} [I_{SRO}^{-1}(\mathbf{k}) - 1], \quad (2.14)$$

the SM interaction differs, at given c and T , only by the constant subtracted from the inverse intensity. Therefore, the off-diagonal direct-space interactions are identical in the KCM and SM approximations.²⁰ However, the KCM formula violates the sum rule (2.1d), thus leading to the appearance of the unphysical self-interaction

$$V_{000}^{KCM} = \frac{T}{2c(1-c)} [\langle I_{SRO}^{-1} \rangle - 1], \quad (2.15)$$

while in the SM, according to Eq. (2.13), this matrix element is zero. Returning to Eq. (2.12), every term in its right-hand side is expressed at this stage in terms of experimental data, and $V_{AE}(\mathbf{k})$ can be easily calculated.

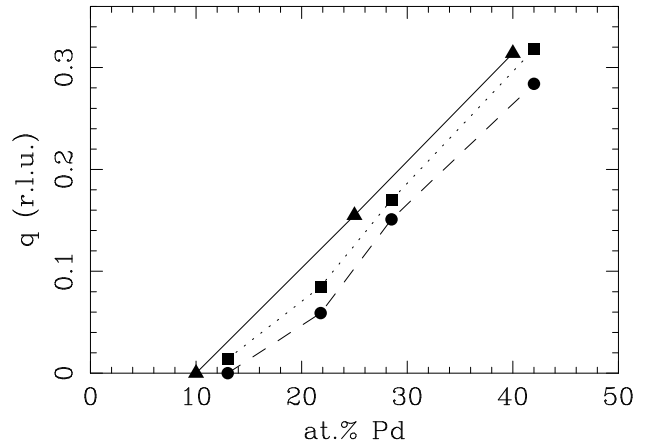


FIG. 2. Concentration dependence of the peak splitting q as measured⁵ in the X-ray diffraction experiment (circles, dashed line) and estimated⁵ from the results of the KKR-CPA electronic-structure calculations²⁷ (squares, dotted line). The data are taken from Table 1 in Ref. 5. The original KKR-CPA results²⁷ (triangles, solid line) are also shown. Straight lines connecting symbols are for the eye guidance only. Note that all the data were originally given in units of the distance between the (000) and (200) positions (equal to 2 r.l.u.) for the separation $m = \sqrt{2} q$ between the adjacent peaks.

III. AVAILABLE DATA

We now consider previously published experimental and theoretical results for equilibrium Cu-Pd alloys in the discussed range of concentrations (20 to 30 at.% Pd). These results are of two types. Firstly, the electron and X-ray diffraction data and the results of the Korringa-Kohn-Rostoker coherent potential approximation (KKR-CPA) electronic-structure calculations are available for the concentration dependence of the peak splitting. Secondly, for several alloy compositions large sets of the SRO parameters were determined by the Fourier inversion of the experimental SRO diffuse scattering intensities. The latter type of data is used as an input for the calculations of the kind described in Sec. II.

The peak separation q was measured at equilibrium for various concentrations and temperatures using electron¹⁻⁴ and X-ray⁵⁻⁷ scattering. The splitting was observed for alloys with more than about 15 at.% Pd, and it increased monotonically with increasing Pd content. Though very good agreement was noted by Gyorffy and Stocks²⁷ (GS) between the electron-diffraction² and their KKR-CPA results, the calculated values of q were systematically slightly higher than the experimental ones. The discrepancy became noticeably larger in more recent measurements. In particular, Saha *et al.*⁵ compared their X-ray results for several compositions with the estimations they made from the GS KKR-CPA calculations.²⁷ They found that the experimental splitting was smaller in all cases. The difference in q ranged from 0.014 to

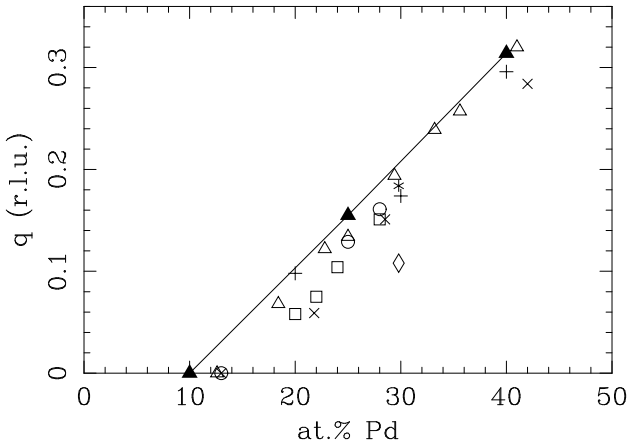


FIG. 3. The same as in Fig. 2, but all available experimental data are presented (Ref. 1 - open squares, ca. 800 K; Ref. 2 - open triangles, 773-893 K; Ref. 3 - open circles, ca. 700 K; Ref. 4 - plusses, 1073 K; Ref. 5 - crosses, 1023 K; Ref. 6 - asterisk, 773 K; Ref. 7 - open diamond, ca. 700 K), in comparison with the KKR-CPA results²⁷ (filled triangles, solid line). The estimations made in Ref. 5 are not shown.

0.034 reciprocal lattice units (r.l.u.); 1 r.l.u. is the distance between the (000) and (100) positions. Their findings (Table 1 in Ref. 5) are shown in Fig. 2, together with the original GS results for different concentrations which were read off Fig. 2 in Ref. 27. Surprisingly, all the estimated values, presumably calculated by interpolating the results of Ref. 27, lie below the GS line; the reason for this is not clear. As a result, the disagreement between the experimental and theoretical values of q is even more pronounced than it was reported in Ref. 5. Fig. 3 compares the KKR-CPA results with the collection of all experimental data for the splitting known to the authors. It is seen that all the experimental points are located below the GS line. We propose an explanation for this discrepancy which is given in Sec. IV.

Sets of the SRO parameters were obtained in the considered concentration interval for 21.8, 28.5 (Ref. 5) and 29.8 (Ref. 6) at.% Pd in X-ray experiments. The samples were annealed at some temperature corresponding to the disordered phase and then quenched. Hereafter these alloys will be referred to according to their numbers in

TABLE I. Data for three Cu-Pd alloys for which sets of the SRO parameters are available: T is the annealing temperature, N_α the number of the SRO parameters in the set, α_{000}^{exp} and q^{exp} the experimental values of α_{000} and q , respectively, q^{rec} corresponds to the recalculated intensity (see text). The splitting q is measured in r.l.u.

No.	at.% Pd	Ref.	T , K	N_α	α_{000}^{exp}	q^{exp}	q^{rec}
1	21.8	5	1023	78	1.018	0.059	0
2	28.5	5	1023	78	1.014	0.151	0
3	29.8	6	773	72	1.786	0.184	0.162

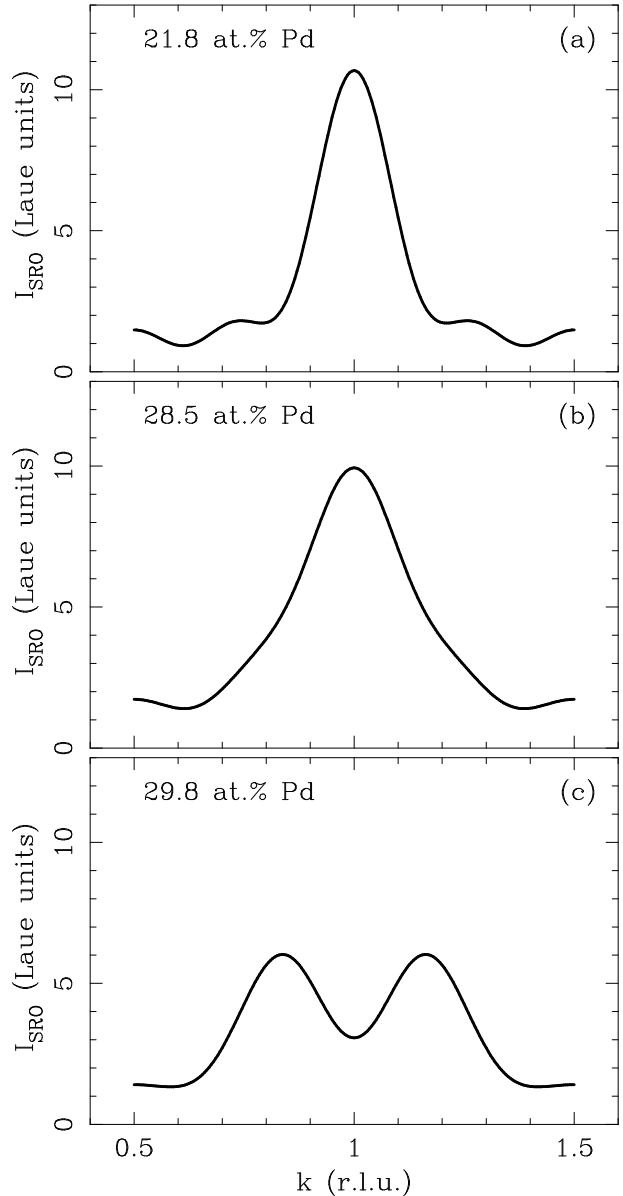


FIG. 4. Profiles of the recalculated SRO diffuse intensities for the alloys 1 (a), 2 (b), and 3 (c) along the (h10) line. Variable k is the component of the wavevector $\mathbf{k} = (k, 1, 0)$. Note that there is no splitting of the (110) peak for the first two alloys.

Table I which contains data used in the subsequent discussion. The splitting of the experimental (110) intensity peak was detected for all three compositions. The SRO parameters for large number of coordination shells were calculated by Fourier-transforming the SRO part of the measured diffuse intensity after having separated it from other intensity contributions. We recalculated the SRO diffuse intensities for these three alloys using tables of the SRO parameters given in Refs. 5 and 6 and the theoretical value $\alpha_{000} = 1$ instead of the experimental values.

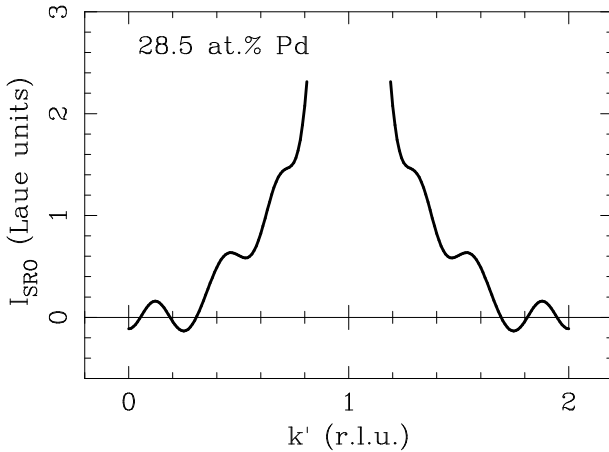


FIG. 5. Recalculated SRO intensity for the alloy 2 along the (h00) line showing ranges of negative values. Variable k' is the component of the wavevector $\mathbf{k} = (k', 0, 0)$.

Such substitution leads to a simple shift of the intensity and does not change its shape. Surprisingly, no splitting of the (110) peak was found in the recalculated SRO intensities for the alloys 1 and 2 (Figs. 4(a) and 4(b)); in the case of the alloy 2 this circumstance has already been noted elsewhere.²⁸ In addition, negative values of the recalculated SRO intensity were found for the alloy 2 (Fig. 5). The origin of all these inconsistencies is probably the insufficient accuracy and/or number of the calculated SRO parameters. Contrary to these two cases, the recalculated SRO intensity for the alloy 3 shows the experimentally observed splitting (Fig. 4(c)). However, the corresponding value of q is noticeably smaller than the experimental result (Table I). As for the first two alloys, we find that the splitting tends to decrease after the recalculation. The accuracy of the recalculated intensity seems to be better for the alloy 3 as far as the magnitude of the splitting is concerned, though the deviation of the integrated intensity α_{000} from unity, which often serves as an accuracy criterion in diffuse-scattering experiments, is much larger than in two other cases (Table I).

IV. RESULTS AND DISCUSSION

We assume that the discrepancy between the experimental and theoretical values of q discussed in Sec. III is the result of the shift of the intensity peak position with respect to the position of the corresponding minimum of the interatomic interaction.¹⁶ In other words, quantities which were measured and calculated were not the same. Indeed, what GS actually calculated²⁷ using the KKR-CPA method were the Fermi surfaces and, in particular, the Fermi wavevectors \mathbf{k}_F along the (110) direction for different concentrations. These Fermi wavevectors were subsequently used to calculate the $2\mathbf{k}_F$ -related separa-

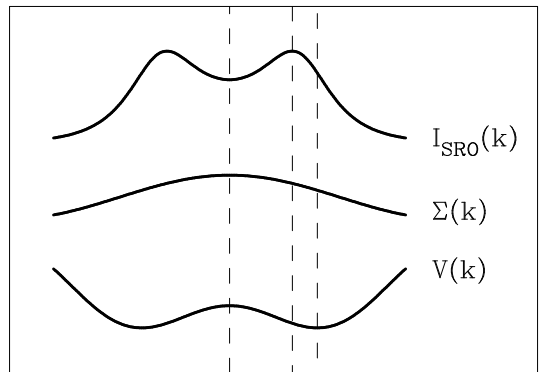


FIG. 6. Shift of the intensity peak position as a result of the wavevector dependence of the self-energy. Behaviour of the SRO intensity, self-energy and interatomic interaction along the (h10) line is shown schematically. The self-energy profile is as found for the three Cu-Pd alloys discussed in the text (see Fig. 8 below). Dashed lines indicate positions (left to right): (110), intensity peak, minimum of the interaction.

tion $m = \sqrt{2}q$ between the adjacent minima of the interaction $V(\mathbf{k})$. Since the mean-field (KCM) description of correlations was chosen, the resulting separation between the intensity peaks was the same. However, it is generally different from the separation between the $V(\mathbf{k})$ minima and depends on temperature because of the temperature-dependent shift of the intensity peak position.¹⁶ The shift itself is the consequence of the wavevector dependence of the self-energy (Fig. 6). This can be easily seen from either Eq. (2.1a) (the direct problem) or Eqs. (2.12), (2.13) (the inverse problem). Consider, e.g., Eq. (2.1a); the $I_{SRO}(\mathbf{k})$ peak positions are determined by the condition $\nabla I_{SRO} = 0$, which leads to

$$2 \nabla V = T \nabla \Sigma , \quad (4.1)$$

while the positions of the $V(\mathbf{k})$ minima are obtained from the equation $\nabla V = 0$. It is clear from Eq. (4.1) that the extrema of $I_{SRO}(\mathbf{k})$ away from the special points are, in general, different from those of $V(\mathbf{k})$. On the other hand, if the approximate self-energy is \mathbf{k} -independent (as in the KCM or the SM approximations), then the two equations coincide and the intensity peak is not shifted. Fig. 3 shows that the KKR-CPA calculations overestimate the experimental peak splitting everywhere in the range of concentrations from 20 to 30 at.% Pd. In the framework of the suggestion about the shift of the $I_{SRO}(\mathbf{k})$ peak being the origin of the disagreement between experiment and theory, this means that the intensity peaks are shifted towards the (110) position.

Based on this assumption, it is now possible to predict the temperature behaviour of the splitting if another, sufficiently reasonable assumption is made. We assume that the temperature dependence of the splitting is always monotonic (a non-monotonic behaviour was never observed experimentally). If this assumption is correct,

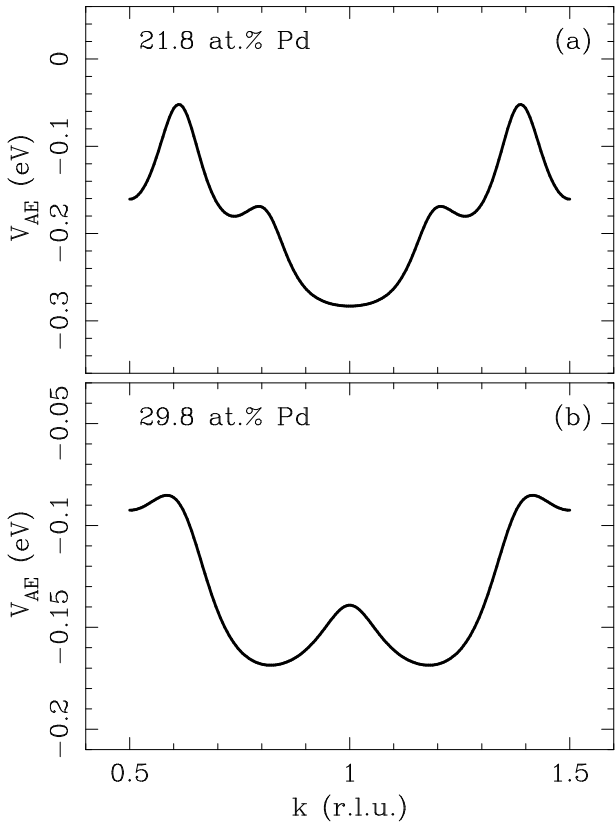


FIG. 7. AE effective pair interactions $V_{AE}(\mathbf{k})$ for the alloys 1 (a) and 3 (b) along the (h10) line.

then the direction of the shift at a particular temperature value can be related to its temperature dependence. At high temperatures corrections to the KCM approximation are small, and the absolute value of the shift tends to zero, decreasing at least as T^{-1} with increasing temperature.¹⁶ Therefore, in the case of the monotonic behaviour of the splitting the direction of the shift is the same at any temperature; the splitting increases with temperature, if the shift is towards the (110) position, and decreases otherwise. For Cu-Pd alloys this would mean that the splitting increases with temperature for all compositions in the considered range. This conclusion is in agreement with the one made on the basis of the inverse temperature hypothesis¹ discussed in Sec. I for alloys with 20, 22 and 24 at.% Pd, but it does not allow the change of the temperature behaviour predicted by this hypothesis for the Cu-28 at.% Pd alloy.

The next step is to check this prediction using the experimental data discussed in Sec. III. These data are quite limited, since sets of the SRO parameters are available only for three compositions. They are also not of sufficient accuracy for the reproduction of the fine structure of the (110) intensity peak. Only in one case, that of the alloy 3, the corresponding set is good enough (i.e., contains sufficient number of the reasonably accurate SRO

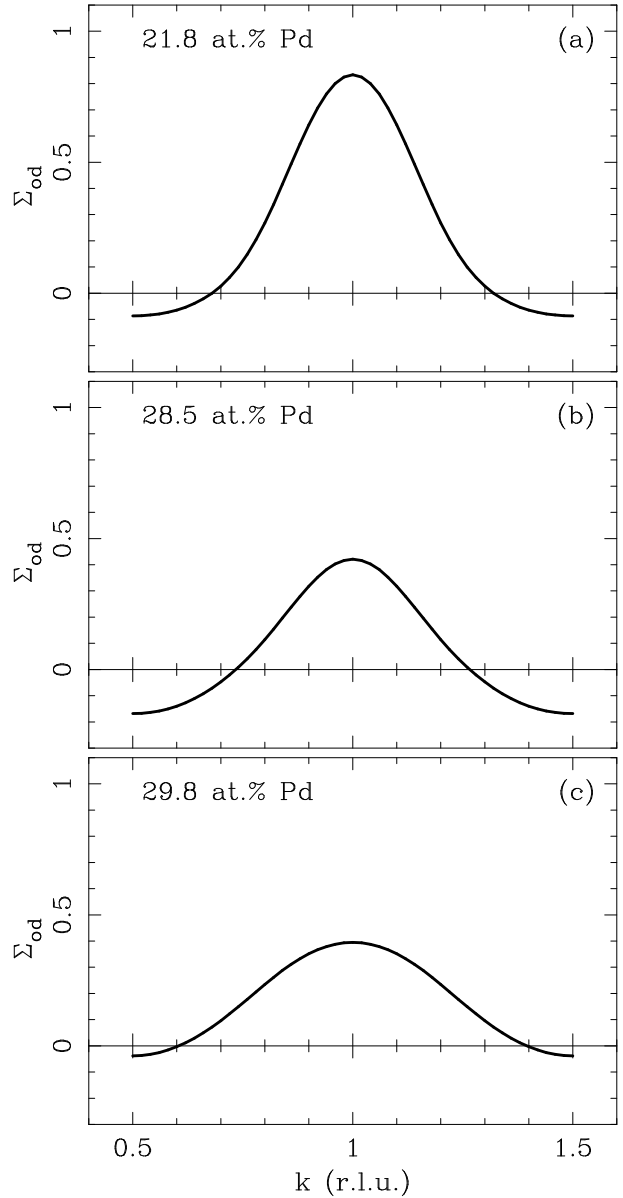


FIG. 8. Profiles of the off-diagonal part $\Sigma_{od}(\mathbf{k})$ of the AE self-energy for the alloys 1 (a), 2 (b), and 3 (c) along the (h10) line. Maximal possible number N_α of coordination shells (Table I) was used in each case.

parameters) to reproduce the experimentally observed splitting in the recalculated diffuse intensity (Fig. 4). Even in this case, the recalculation changes noticeably the magnitude of the splitting (see Table I). It seems that in this particular situation of the split intensity peaks even larger sets of the more accurately determined SRO parameters are necessary. Nevertheless, the available sets can still be used to obtain information about the temperature dependence of the peak separation. The straightforward approach to this task described in Sec. II is applicable only to the alloy 3. The solution of the in-

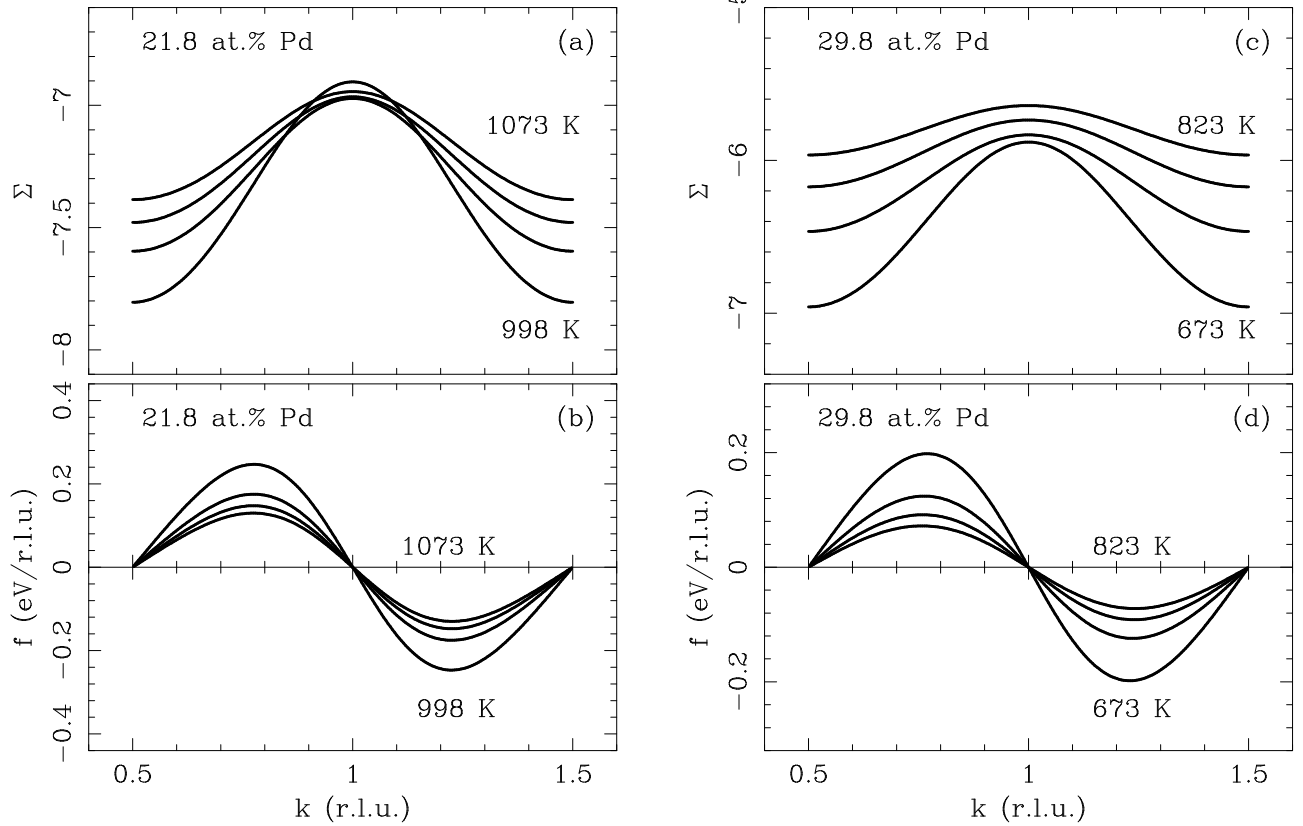


FIG. 9. AE self-energy $\Sigma(k)$ (a,c) and the related function $f(k)$ defined by Eq. (4.2) (b,d) for the alloys 1 (a,b) and 3 (c,d) along the (h10) line at several equidistant temperatures. Indicated are maximal and minimal temperatures; the temperature steps are 25 K (a,b) and 50 K (c,d). The KCM values for the self-energy (Eq. (4.3)) are $\Sigma^{KCM} = -5.87$ (a) and $\Sigma^{KCM} = -4.78$ (c).

verse diffuse scattering problem given by Eqs. (2.12) and (2.13) cannot be obtained for the alloy 2, because the recalculated diffuse intensity becomes negative (Fig. 5); in this case the inverse intensity $I_{SRO}^{-1}(\mathbf{k})$ and, therefore, the effective interatomic interaction $V_{AE}(\mathbf{k})$ would contain unphysical singularities at those positions in the \mathbf{k} -space where the diffuse intensity vanishes. The inverse problem can be solved for the alloy 1, for which the recalculated intensity is always positive. However, in this case the resulting interaction which follows the shape of the intensity does not have a split minimum at the (110) position. The profiles of $V_{AE}(\mathbf{k})$ for the alloys 1 and 3 are shown in Fig. 7.

The easiest quantity to calculate in the framework of the AE theory of SRO is the direction of the shift. This can be done for all three alloys, despite problems with the data for two of them as indicated before. According to Eq. (4.1), the direction of the shift is determined by the reciprocal-space behaviour of the self-energy, and the latter can be easily obtained by Fourier-transforming Eq. (2.1c), i.e., calculating $\Sigma_{od}(\mathbf{k})$, and using the experimental values of the SRO parameters. It is expected that the off-diagonal part of the self-energy is much less sensi-

tive to the accuracy of the $\{\alpha_{lmn}\}$ set than the profile of the split intensity peak itself; there is no special reason for the self-energy to have any extrema away from the special points. Also, Σ_{od} is of the second order in α_{lmn} (Eq. (2.1c)) and therefore decreases in the direct space faster than the PCF, which means that the distant SRO parameters are less important for its calculation. The results of such calculation are presented in Fig. 8. The convergence of the results with respect to the number of coordination shells included in the AE approximation improves rapidly with increasing concentration; to achieve very good convergence, about 40, 20 and 5 shells are necessary for the alloys 1, 2 and 3, respectively. In all three cases $\Sigma_{od}(\mathbf{k})$ has a maximum at the (110) position, and from Eq. (4.1) it follows that the intensity peaks are shifted towards this position (see Fig. 6). This result is in agreement with our interpretation of the discrepancy between the experimental and the KKR-CPA values of q .

The actual value of the shift can be calculated only for the alloy 3, since for the other two alloys positions of neither peaks of the recalculated intensity nor minima of the AE interaction are available. The 10-shell AE approximation was used for this and all other calcula-

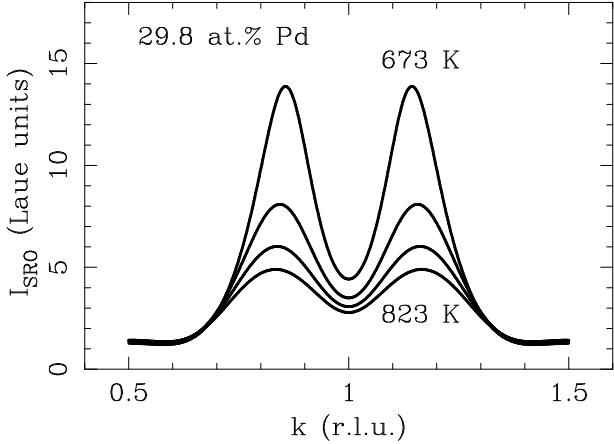


FIG. 10. AE intensity profiles for the alloy 3 along the (h10) line at several equidistant temperatures. The temperature range and step are as in Figs. 9(c) and 9(d).

tions discussed in the rest of the paper. The result is 0.018 r.l.u.; it should be compared with the deviations of the experimental points from the GS line in Fig. 3. The deviation for the alloy 3 calculated by the linear interpolation of the GS results is 0.022 r.l.u., which is very close to the result obtained in the AE calculation. If we assume that the AE shift is about the same for both the experimental and recalculated intensities, then the position of the $V_{AE}(\mathbf{k})$ minimum for the former just falls on the GS line. The deviations of other experimental points are of the same order of magnitude.

The change of the splitting with temperature can be analysed for the two cases (alloys 1 and 3) in which the inverse problem can be solved. This is done by calculating the self-energy as a function of temperature. Let us consider the profile of the self-energy along the (h10) line. Along this line the self-energy is a function of just one component k of the wavevector $\mathbf{k} = (k, 1, 0)$. We define a function

$$f(k) = T \frac{\partial \Sigma}{\partial k}, \quad (4.2)$$

the temperature dependence of which, according to Eq. (4.1), determines that of the splitting. The functions $\Sigma(k)$ and $f(k)$ at different temperatures for the two alloys are displayed in Fig. 9. Accuracy checks show that the 10-shell approximation works very well for the alloy 3 and is still satisfactory (though noticeably worse) in the case of the alloy 1. Note that the AE results for the self-energy differ considerably from its KCM values; the KCM expression for the self-energy can be obtained, e.g., from the comparison of Eqs. (2.9) and (2.14):

$$\Sigma^{KCM} = -\frac{1}{c(1-c)}. \quad (4.3)$$

In both cases the absolute value of $f(k)$ decreases with increasing temperature for any given value of k , which

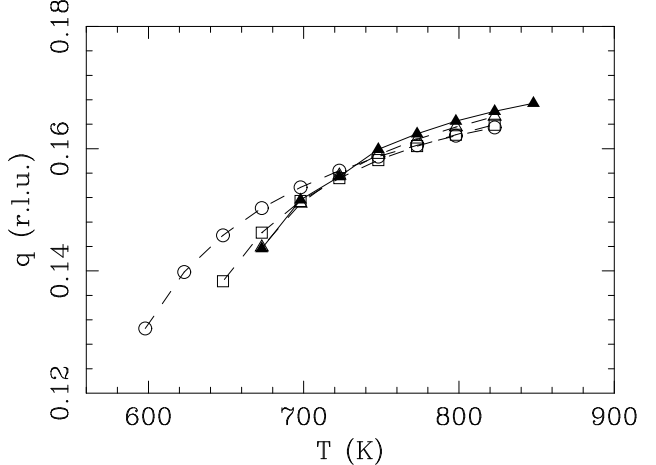


FIG. 11. Intensity peak position q as function of temperature for the alloy 3 (filled triangles, solid line). Results for three other compositions (open symbols, dashed lines), 20 (circles), 24 (squares) and 28 (triangles) at.% Pd, calculated using the same AE interaction are also shown.

corresponds to the increase of the splitting with temperature. This result agrees with the conclusion based on the assumption of the monotonic temperature dependence of the splitting which was made earlier in this Section.

Finally, a quantitative calculation of the temperature dependence of the intensity peak position q can be carried out, as before, for only one composition (alloy 3). The corresponding intensity profiles are presented in Fig. 10, while Fig. 11 shows results for the function $q(T)$ for this composition, as well as for three other concentrations covering the interval which was considered in Ref. 1. In all calculations the same AE interaction (namely, that obtained by solving the inverse problem for the alloy 3; see Fig. 7(b)) was used. The aim was to find out whether the variation of composition for the same interaction would lead to any particular change of the function $q(T)$. No such change takes place, as it is seen from Fig. 11; the splitting increases monotonically with temperature for all four alloy concentrations.

In summary, we studied theoretically the temperature dependence of the Fermi surface-induced splitting of the (110) SRO diffuse intensity peak for Cu-Pd alloys under equilibrium conditions. The comparison was made with experimental observations for these alloys in a steady state under irradiation. The validity of the inverse temperature hypothesis proposed previously to relate the two regimes was examined. At equilibrium this hypothesis predicts the qualitative change of temperature behaviour near the Cu_3Pd composition, namely, the increase of the splitting with increasing temperature in the composition interval 20 to 24 at.% Pd and its decrease with temperature as the concentration of Pd increases to 28 at.%. Comparing available electron and X-ray scattering data with the results of the KKR-CPA electronic-structure

calculations, we found that the theoretical approach overestimated the experimental splitting. This disagreement was interpreted as the result of the shift of the diffuse intensity peaks with respect to the positions of the corresponding minima of the effective pair interatomic interaction towards the (110) position. An additional assumption about monotonicity of the temperature dependence of the splitting led to a connection between the direction and temperature behaviour of the peak shift. Under this assumption the shift towards the (110) position is equivalent to the increase of the splitting with increasing temperature. For Cu-Pd alloys this means that the splitting increases with temperature for all concentrations in the considered compositional range. This conclusion seems to be confirmed by the AE calculations, which are, however, based on limited experimental data. It agrees with the prediction of the inverse temperature hypothesis for lower Pd concentrations (20 to 24 at.%) but, contrary to this prediction, does not allow any reversal of the temperature behaviour with increasing concentration of Pd. It also contradicts the results of recent computer simulations¹⁷ and X-ray measurements⁷ for higher Pd content (25 and 29.8 at.%, respectively), according to which the splitting is (almost) temperature-independent. These results are consistent, on the other hand, with the reversal scenario. Among possible reasons for this disagreement are (i) limited validity of the inverse temperature hypothesis, (ii) insufficient accuracy and/or size of the available sets of the experimental SRO parameters, (iii) pair character of the interatomic interactions used in the AE theory of SRO and (iv) approximate character of the AE calculations. Further direct measurements of the splitting as a function of temperature (as in Ref. 7) at the discussed range of compositions are necessary to clarify the situation.

The authors would like to thank H. Reichert and collaborators for communicating their experimental results (Ref. 7) prior to publication.

- ⁸ M.A. Krivoglaz, *Theory of X-Ray and Thermal Neutron Scattering by Real Crystals* (Plenum, New York, 1969); *Diffuse Scattering of X-Rays and Neutrons by Fluctuations* (Springer, Berlin, 1996).
- ⁹ S.C. Moss, Phys. Rev. Lett. **22**, 1108 (1969); S.C. Moss and R.H. Walker, J. Appl. Crystallogr. **8**, 96 (1974);
- ¹⁰ P.C. Clapp and S.C. Moss, Phys. Rev. **142**, 418 (1966); **171**, 754 (1968).
- ¹¹ A. Finel and D. de Fontaine, J. Statist. Phys. **43**, 645 (1986).
- ¹² H. Reichert, S.C. Moss, and K.S. Liang, Phys. Rev. Lett. **77**, 4382 (1996).
- ¹³ S.C. Moss and H. Reichert (private communication).
- ¹⁴ H. Reichert, I. Tsatskis, and S.C. Moss, in *Proceedings of the Joint NSF/CNRS Workshop on Alloy Theory, Mont Sainte Odile Monastery, Strasbourg, France, October 11-15, 1996*, Comput. Mater. Sci. **8**, 46 (1997).
- ¹⁵ H. Roelofs, B. Schönfeld, G. Kostorz, W. Bührer, J.L. Robertson, P. Zschack, and G.E. Ice, Scripta Mat. **34**, 1393 (1996).
- ¹⁶ I. Tsatskis, preprint cond-mat/9801089 (to be published).
- ¹⁷ V. Ozoliņš, C. Wolverton, and A. Zunger, Phys. Rev. Lett. **79**, 955 (1997).
- ¹⁸ V.I. Tokar, Phys. Lett. A **110**, 453 (1985).
- ¹⁹ V.I. Tokar, I.V. Masanskii, and T.A. Grishchenko, J. Phys.: Condens. Matter **2**, 10199 (1990).
- ²⁰ I.V. Masanskii, V.I. Tokar, and T.A. Grishchenko, Phys. Rev. B **44**, 4647 (1991).
- ²¹ E.g., F. Ducastelle, *Order and Phase Stability in Alloys* (North-Holland, Amsterdam, 1991).
- ²² E.g., Yu.A. Izyumov and Yu.N. Skryabin, *Statistical Mechanics of Magnetically Ordered Systems* (Consultants Bureau, New York and London, 1988).
- ²³ I. Tsatskis, in *Local Structure from Diffraction*, Fundamental Materials Science Series, edited by M.F. Thorpe and S.J.L. Billinge (Plenum Press, New York, 1998, in press).
- ²⁴ L. Reinhard and S.C. Moss, Ultramicroscopy **52**, 223 (1993); M. Borici-Kuqo and R. Monnier, Ref. 14, p. 16; D. Le Bolloc'h, T. Cren, R. Caudron and A. Finel, Ref. 14, p. 24.
- ²⁵ G.S. Joyce, in *Phase Transitions and Critical Phenomena*, Vol. 2, eds. C. Domb and M.S. Green (Academic Press, New York, 1972); R. Brout, *Phase Transitions* (Benjamin, New York, 1965).
- ²⁶ L. Onsager, J. Am. Chem. Soc. **58**, 1468 (1936); J.B. Staunton and B.L. Gyorffy, Phys. Rev. Lett. **69**, 371 (1992).
- ²⁷ B.L. Gyorffy and G.M. Stocks, Phys. Rev. Lett. **50**, 374 (1983).
- ²⁸ Z.W. Lu, D.B. Laks, S.-H. Wei, and A. Zunger, Phys. Rev. B **50**, 6642 (1994).

[†] Former name: I. V. Masanskii

¹ J. Kulik, D. Gratias, and D. de Fontaine, Phys. Rev. B **40**, 8607 (1989).

² K. Ohshima and D. Watanabe, Acta Cryst. A **29**, 520 (1973).

³ D. Watanabe, J. Phys. Soc. Jpn. **14**, 436 (1959).

⁴ M. Rodewald, K. Rodewald, P. De Meulenaere, and G. Van Tendeloo, Phys. Rev. B **55**, 14173 (1997).

⁵ D.K. Saha, K. Koga, and K. Ohshima, J. Phys. Condens. Matter **4**, 10093 (1992).

⁶ K. Ohshima, D. Watanabe, and J. Harada, Acta Cryst. A **32**, 883 (1976).

⁷ H. Reichert, H.H. Hung, V. Jahns, K.S. Liang, D. Zehner, and H. Dosch (to be published).